Enhanced low band MIMO terminal antenna based on selective feeding of chassis modes

Aliakbari Abar, Hanieh; Liang, Qiuyan; Lau, Buon Kiong

Published in:
14th European Conference on Antennas and Propagation (EuCAP)

DOI:
10.23919/EuCAP48036.2020.9135391

2020

Document Version:
Peer reviewed version (aka post-print)

Enhanced Low Band MIMO Terminal Antenna Based on Selective Feeding of Chassis Modes

Hanieh Aliakbari[1], Qiuyan Liang[1,2], Buon Kiong Lau[1]
[1] Department of Electrical and Information Technology, Lund University, Lund, Sweden, hanieh.aliakbari_abar@eit.lth.se
[2] National Key Laboratory of Antennas and Microwave Technology, Xidian University, Xi'an, China

***Abstract*—Multiple-input multiple-out (MIMO) is a mature technology in modern wireless communications. However, it is challenging to implement multi-antennas for MIMO operation in compact mobile terminals, due to high mutual coupling and correlation among closely spaced antenna elements. Moreover, a conventional terminal chassis only offers one resonant mode below 1 GHz, complicating multi-antenna design. Recently, it has been shown that the chassis can be modified to facilitate a few resonant modes below 1 GHz. However, attempts to excite these modes selectively using a single coupling feed per antenna port result in limited bandwidth and isolation. In this work, we propose dual-feed antenna ports to improve selective feeding of the resonant modes of an existing two-port MIMO terminal antenna below 1 GHz. Simulation results reveal significantly enhanced bandwidths of 30% and 15% for the two ports, as well as high isolation of over 32 dB.**

***Index Terms*—MIMO systems, terminal antennas, feed design, characteristic modes.**

I. Introduction

Multiple-input multiple-out (MIMO) technology is very popular due to its ability to provide high spectral efficiency in wireless communications [1]. However, to implement MIMO in terminal antennas is challenging, as their compact form factor leads to the multi-antennas being placed in close proximity to one another [2]. Moreover, at frequencies below 1 GHz, the terminal chassis can only provide one resonant characteristic mode (CM), which limits the ability of multi-antennas to simultaneous provide sufficient bandwidth and isolation for practical mobile applications [3].

To increase bandwidth while retaining good isolation, it is shown that the resonant frequency of the chassis' higher order modes can be tuned to below 1 GHz, by slightly modifying the chassis [3]-[5]. For example, the new modes enable the chassis-based MIMO antenna in [3] to not only cover LTE Bands 5 (824-894 MHz) and 8 (880-960 MHz) using the main antenna, but also Band 8 for the second antenna [3]. However, the 6 dB impedance bandwidths (20% and 9%, respectively) are still limited and the simulated isolation is as low as 8.5 dB near the upper band edge.

In this work, we propose to use more capacitive coupling elements (CCEs) to improve the bandwidth and isolation of the MIMO terminal antenna proposed in [3]. In particular, two CCEs are used for each antenna port to excite the desired mode selectively. This is to prevent any port from exciting the mode used by the other port, resulting in isolation of over 32 dB in the operating band. Moreover, the multi-CCE design that facilitates selective excitation also enhances the bandwidth of the two ports to 30% and 15%, respectively. This result confirms a previous study on the beneficial effect of increasing the number of coupling elements on bandwidth with selective excitation [6].

Selective excitation of CMs using multiple coupling elements has been investigated for MIMO terminal antennas [7], [8]. However, earlier studies focus on higher frequencies (above 2 GHz), where multiple resonant modes are inherent to the terminal chassis and the outputs from the same CCEs are combined differently to excite different CMs. The subject of bandwidth improvement was not investigated.

In addition, it is noted that, instead of selective excitation, multiple coupling elements have also been used to increase the bandwidth of a single-antenna for vehicular application by simultaneously exciting multiple resonant modes [9].

II. Characteristic Mode Analysis

A. CMs of Conventional and Modified Terminal Chassis

For the purpose of antenna design, a conventional chassis can often be represented by a rectangular perfect electric conductor (PEC) plate of zero thickness. A typical chassis size is 120 mm × 60 mm. In [3], it is shown that adding shorted PEC strips along the longer sides results in capacitive loading that introduces two additional resonant CMs below 1 GHz. Accordingly, two loading strips of the height of 5 mm and the length of 120 mm are added 5 mm above the longer edges of the plain chassis (see Fig. 2). Two shorting strips (0.5 mm in width) are added at the center of the two loading strips. The first three resonant CMs of the modified chassis are shown in Fig. 1 for the frequency range from 0.6 to 1.2 GHz. The conventional chassis only provides one resonant CM in this frequency range and its eigenvalue is almost identical to that of mode 1 in Fig. 1. The CM analysis was performed using the method-of-moment solver of 2018 Altair FEKO (version 2018.2.1).

As explained in [3], modes 1 and 2 of the modified chassis are the fundamental dipole mode and the cross dipole mode, respectively. Therefore, the electric fields of mode 1 is maximum around the two shorter sides with a phase difference of 180° (see Fig. 2(a)). Correspondingly, the electric fields of mode 2 is maximum around the two shorter sides with a phase difference of 180° (see Fig. 2(b)).

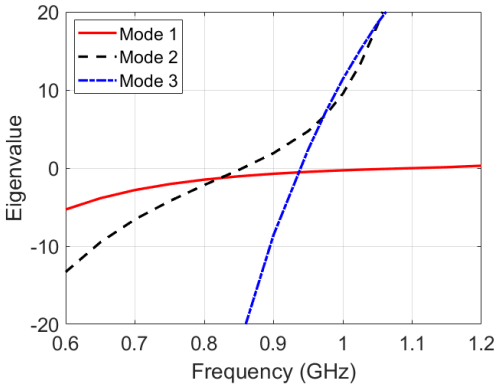

Fig. 1. Characteristic eigenvalues of the first three resonant modes of the modified chassis.

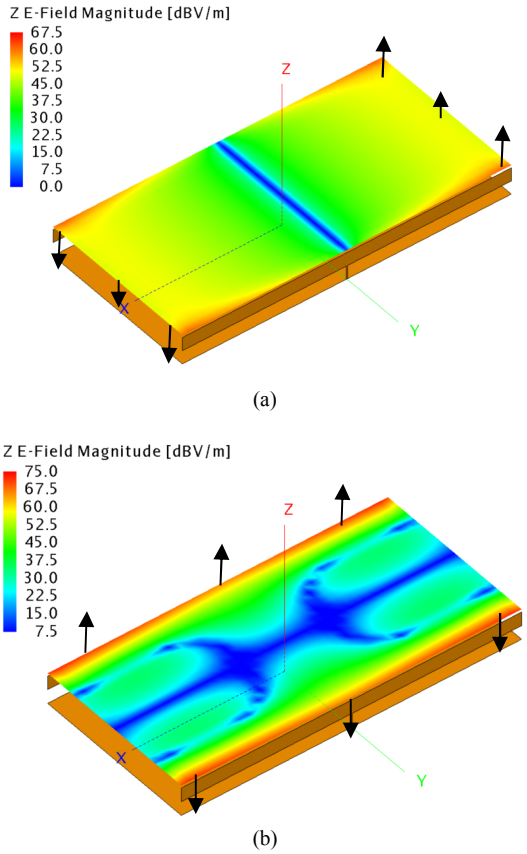

(a) (b)

Fig. 2. Magnitude and phase of z-oriented electric fields of (a) modes 1 and (b) mode 2, 11 mm above the modified chassis. The black arrows indicate the magnitude and phase of the fields along the shorter and longer sides.

B. *Dual-CCE Feed Design*

For the modified chassis in [3], which is similar to the modified chassis in this work, a self-resonant element is used for port 1 to excite mode 1. Port 2 consists of a CCE placed next to shorting strip, to excite mode 2. These feeding positions were chosen based on the modal electric field distributions shown in Fig. 2. However, the single-element or single-CCE feed solution suffers from leakage of power into

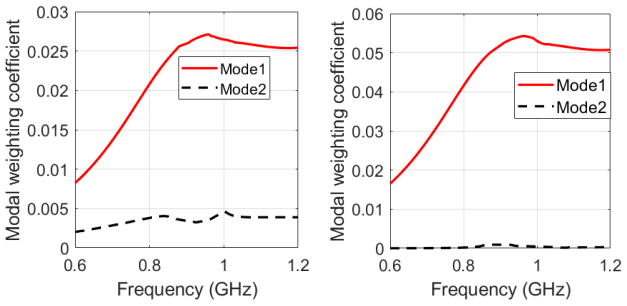

(a) (b)

Fig. 3. Modal weighting coefficients for port 1 with (a) single-feed and (b) dual-feed designs.

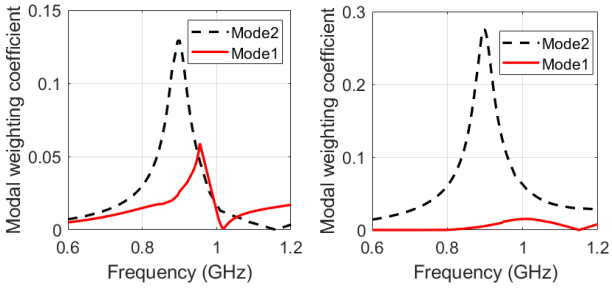

(a) (b)

Fig. 4. Modal weighting coefficients for port 2 with (a) single-feed and (b) dual-feed designs.

other mode(s), due to the electric fields of other modes not being perfectly zero at the feed point chosen to excite a desired mode. One direct consequence of leakage power is that the isolation of the dual-port design in [3] is as high as 8.5 dB at the upper band edge.

To illustrate the leakage effect, the modal weighting coefficient for port 1 excitation with a single-CCE (instead of a self-resonant element in [3]) is shown in Fig. 3(a). As can be seen, mode 2 is significantly excited by port 1. To provide some clearance between the CCE and the nearby loading strip for this simulation, the two loading strips are shifted along the chassis edge towards the other shorter side of the chassis, as depicted in Fig. 5. Nevertheless, the loading strips still have an effect on the matching of the CCE. Moreover, only one CCE at the shorter side was excited (the other three CCEs were present but not fed). Similarly, port 2 in [3] is equipped with only one CCE element, with the intention to only excite mode 2. The simulation model for this case is identical to Fig. 5, but with only one CCE located beside a shorting strip being fed (by port 2). The modal weighting coefficient in Fig. 4(a) illustrates the significant contribution from mode 1 in the excitation of port 2, especially in the vicinity of 0.95 GHz.

To more efficiently and selectively excite modes 1 and 2 using ports 1 and 2, respectively, dual-CCEs can be used for each port. For port 1, as guided by Fig 2(a), two small CCEs can be placed along one shorter side of the chassis, as performed in the single-port antenna design in [6]. This configuration is illustrated in Fig. 5. These two CCEs were

fed in phase by port 1, which not only increased the excitation of mode 1 (as evidenced by the larger modal weighting coefficient), but they also prevented mode 2 from being excited, due to the electric field of mode 2 being out of phase across the shorter side. As also shown in [6], using four CCEs on the other side of the chassis with proper excitation phase shift will further increase the modal weighting coefficient and the bandwidth of port 1. However, for the current design shown in Fig. 5, only two CCEs are used. The resulting modal weighting coefficient in Fig. 3(b) shows that mode 2 is effectively suppressed. In other words, very little power is coupled into mode 2 from port 1.

On the other hand, selective excitation of mode 2 by port 2 is achieved by placing two CCEs with out-of-phase excitation near the two shorting pins of the loading strips (see Fig. 5). This is motivated by the out-of-phase electric field of mode 2 across the width of the chassis, as well as the in-phase electric field of mode 1 across the width. As shown in Figs. 4(b), mode 2 is now excited by port 2 with a larger modal weighting coefficient, whereas modes 1 is well suppressed by the out-of-phase dual-CCE feed design.

III. Antenna Performance

A. MIMO Antenna and Circuit Design

Following the discussion in the previous section, the proposed MIMO antenna with four CCEs were incorporated onto the modified chassis (two CCEs for each port). Relevant parameters were optimized to yield better performance. For example, when all CCEs were included in the model, the characteristic eigenvalues were slightly shifted due to the additional structural loading. The final design is illustrated in Fig. 5 and the relevant parameter values are listed in the figure caption. As for the CM analysis, the entire structure was assumed to be PEC. It is noted that by adding all the CCEs to the integrated structure, the resonant frequency of mode 2 will be slightly increased (see Fig. 7) and this deviation can be compensated by either folding (see Fig. 5) or meandering the loading strip (see Fig. 6). Figure 7 also shows how mode 2 evolves as the CCEs and loading strips are progressively added in Cases 1 to 4.

To facilitate impedance matching for the dual-port MIMO terminal antenna that relies on non-resonant CCEs for modal excitation, the BetaMatch software was used to design the matching network. Moreover, a power combiner is needed to combine the signal from the CCEs at each port. For port 2, the out-of-phase excitation across the two CCEs is provide by a 180° phase shifter. The schematic of the matching network is given in Fig. 6 and the parameter values are provided in Table 1.

B. MIMO Antenna Performance

The full-wave antenna simulation was performed using 2018 CST time-domain solver, since it provides a convenient platform for circuit co-simulation.

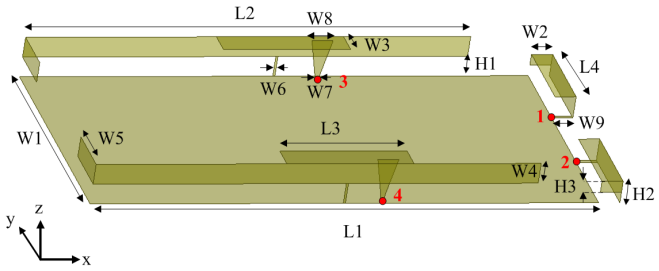

Fig. 5. Final design with the optimized dimensions (L_1 = 115 mm, L_2 = 105 mm, L_3 = 30 mm, L_4 = 20 mm, W_1 = 60 mm, W_2 = 5 mm, W_3 = 6 mm, W_4 = 5 mm, W_5 = 13 mm, W_6 = 0.5 mm, W_7 = 1 mm, W_8 = 5 mm, W_9 = 5 mm, H_1 = 5 mm, H_2 = 5.4 mm, H_3 = 2.7 mm). The location of the excitation ports 1-4 at the CCEs are indicated with small red dots.

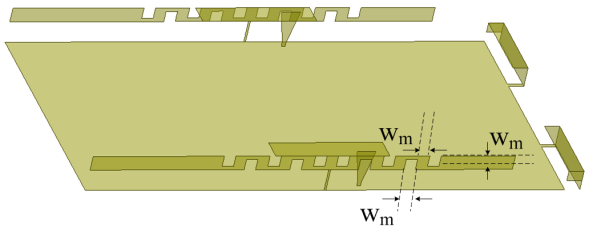

Fig. 6. Alternative design using meandered strips. The dimensions are the same as Fig. 5 apart from the meandered strip parameters (W_m=3 mm) and the removal of the folded parts of the strips.

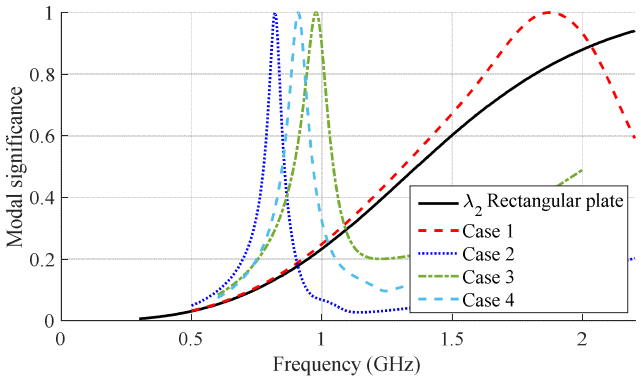

Fig. 7. Modal significance of mode 2 for the rectangular plate, *Case 1*: Rectangular plate with two CCE in the edge, *Case 2*: Case 1 with two strip along the longer side, *Case 3*: Case 2 with two CCEs along the longer sides, *Case 4*: Case 3 with two meandered strip along the longer side.

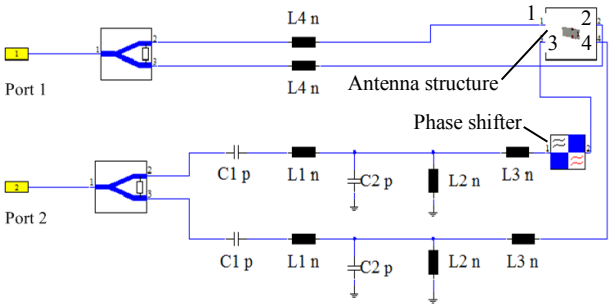

Fig. 8. Matching network, phase shifter and combiner for the proposed two-port antenna. The antenna structure is represented by a block with its four excitation ports at the CCEs.

Table.1. Parameters of inductances and capacitances in matching network.

C1	C2	L1	L2	L3	L4
14.81pF	3.51pF	23.3nH	43.3nH	8.2nH	27nH

The scattering parameters of the two-port MIMO antenna is shown in Fig. 9. As can be seen, the selective excitation provides the 6 dB impedance bandwidth of 0.78-1.1 GHz (30%) at port 1. This bandwidth is significantly larger than that achieved by port 1 in [3] (20%) and the two CCEs are smaller than the self-resonant element used by port 1 in [3]. This result is obtained due to more efficient excitation of mode 1 by two in-phase CCEs. Similarly, the bandwidth of port 2 (0.83-0.97 GHz, or 15%) is significantly larger than the 9% bandwidth of port 2 in [3]. This is again obtained because of the larger weighing coefficient enabled by the two CCEs.

Given the selective excitation of the desired mode by each of the two ports, as shown in Figs. 3(b) and 4(b), good isolation performance can be expected. Indeed, Fig. 9 shows that the achieved isolation to be above 32 dB over the operating frequency band.

The 3D farfield patterns of the two ports at 0.9 GHz are plotted in Fig. 10. As expected, the patterns of ports 1 and 2 are those of the fundamental dipole mode (mode 1) and the cross dipole mode (mode 2), respectively. In other words, the modes are selectively excited by these antenna ports. In Fig. 11, the envelope correlation coefficient (ECC) of the proposed antenna is shown, assuming 3D uniform angular power spectrum. The ECC was calculated from the far-field patterns of the two-port MIMO antenna. The ECC is very low over the operating band (around 0.002 at the highest point), which is desirable for efficient MIMO performance.

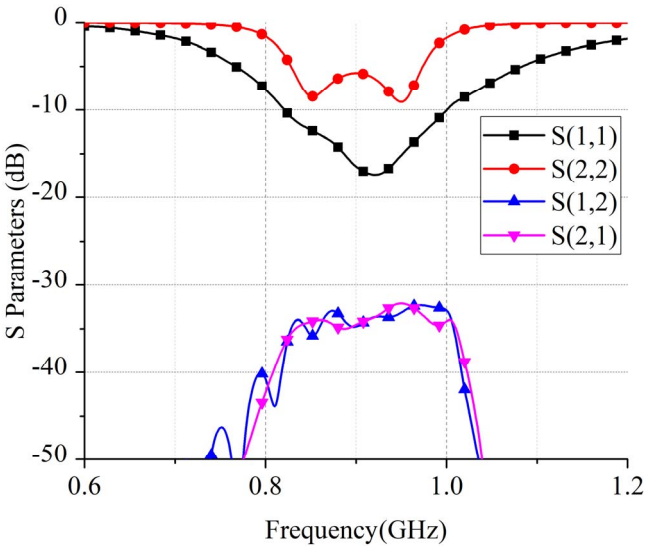

Fig. 9. Scattering parameters of the proposed two-port MIMO antenna.

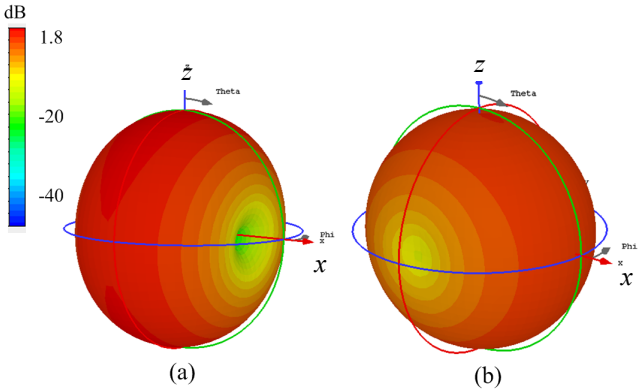

Fig. 10. 3D farfield gain patterns of the proposed two-port MIMO antenna at 0.9 GHz.

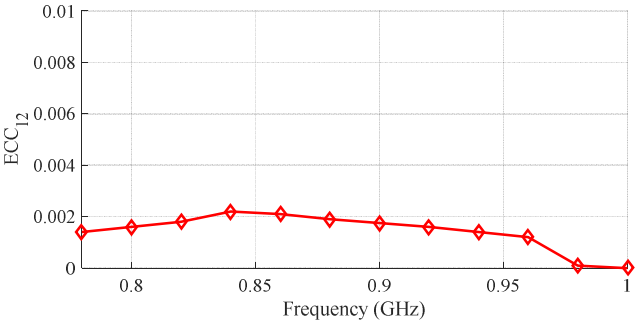

Fig. 11. ECC of the proposed two-port MIMO antenna.

IV. Conclusions

This work shows that the use of multiple coupling elements for selective modal excitation is highly beneficial for MIMO antenna design from the perspective of bandwidth and isolation enhancement. Naturally, having more than one coupling element for each antenna port increases the overall antenna footprint, and the use of power combiner and potentially more complicated matching network can incur higher cost and complexity, as well as higher power loss. However, the results in [6] also show that more coupling elements can also require fewer matching elements, to achieve a given bandwidth. This is an interesting aspect for future work.

Acknowledgment

This work is supported by the Swedish Research Council under Grant no. 2010-468 and 2018-04717.

References

[1] M. A. Jensen and J. W. Wallace, "A review of antennas and propagation for MIMO wireless communications," *IEEE Trans. Antennas Propag.*, vol. 52, no. 11, pp. 2810–2824, Nov. 2004.

[2] H. Li and B. K. Lau, "MIMO systems and antennas for terminals," in *Handbook of Antenna Technologies*, Z. N. Chen, Ed. Springer, 2015, pp. 1-35.

[3] H. Li, Z. Miers, and B. K. Lau, "Design of orthogonal MIMO handset antennas based on characteristic mode manipulation at frequency bands below 1 GHz," *IEEE Trans. Antennas Propag.*, vol. 62, no. 5, pp. 2756-2766, May 2014.

[4] Z. Miers, H. Li, and B. K. Lau, "Design of bandwidth enhanced and multiband MIMO antennas using characteristic modes," *IEEE Antennas Wireless Propag. Lett*., vol. 12, pp. 1696-1699, 2013.

[5] Z. Miers, H. Li, and B. K. Lau, "Design of bezel antennas for multiband MIMO terminals using characteristic modes," in *Proc. 8th Europ. Conf. Antennas Propag. (EuCAP'2014)*, The Hague, The Netherlands, Apr. 6-10, 2014, pp. 2556-2560.

[6] H. Aliakbari and B. K. Lau, "'On modal excitation using capacitive coupling elements and matching network'," in *Proc. IEEE Int. Symp. Antennas Propag. (APS'2019)*, Atlanta, GA, Jul. 7-12, 2019

[7] R. Martens, E. Safin, and D. Manteuffel, "Inductive and capacitive excitation of the characteristic modes of small teminals," in *Proc. Loughborough Antennas Propag. Conf. (LAPC)*, Loughborough, UK, Nov. 14-15, 2011.

[8] D. Manteuffel and R. Martens, "Multiple antenna integration in small terminals," in *Proc. Int. Symp. Antennas Propag. (ISAP'2012)*, Nagoya, Japan, Oct. 29-Nov. 2, 2012.

[9] R. Ma, T. Y. Shih, R. Lian, and N. Behdad, "Design of bandwidth-enhanced platform-mounted electrically small VHF antennas using the characteristic-mode theory," *IEEE Antennas Propag. Lett*., vol. 17, no. 2, pp. 2384-2388, 2017.